International Journal of Future Generation Communication and Networking
Vol. 14, No. 1, (2021), pp. 1307–1319

An Eye Ailment Appreciation Scheme from Bacterial Infective Diseases Using Machine Learning Techniques

Janet Grace Susila.S[1], Dr.D.Kavitha[2]
[1]Research Scholar, Department of Computer Science and Applications, St.Peter's Institute of Higher Education and Research, Chennai, India
[2]Associate Professor, Department of Computer Science and Application,St.Peter's Institute of Higher Education and Research, Chennai, India
janetinba1980@gmail.com
d.kavithamoorthy@gmail.com

Abstract

Infectious keratitis is the most common entities of corneal diseases, in which pathogen produce in the cornea leading to softness and destroying of the corneal tissues. Infectious keratitis is a medical emergency, for which a fast and accurate diagnosis is needed fortroy speedy initiation of prompt and simple treatment to cure the disease progress and to reduce the extent of corneal damage; otherwise it may develop sight-threatening and even is eye-globe-threatening condition. In this paper, infectious corneal disease is the classification of clinical images. The assinged system automatically divides the countance components from the frontal facial image and extracts the eye part. The proposed method analyzes and classifies peri-orbital cellulitis, and Bitot's spot of vitamin A deficiency. From the experimental results, we see that the DCNNmodel outperforms SVM models. We also compare our method with some other existing methods. Our process shows improved accuracy compared to other process. The average accuracy rate of our DCNN model is 98.79% with sensitivity of 97% and specificity of 99%.

Key words: *Deep convolution neural network, support vector machine digital image processing , principal component analysis, t-distributed stochastic neighbor embedding, automated eye disease recognition.*

1. Introduction

The disease that affects the cornea is the leading cause of corneal blindness. One of the major causes of corneal blindness is corneal ulcer [1]. The corneal ulcer detection and segmentation is still a submissive work due to detect its ulcer location, size measurement, and visualacuity. However, theesegmentation part of corneal ulcer depends on doctor of medicine and through experience It provides different segmentation results because of doctor of medicine different professional knowledge and also less time period needed Therefore, how to cope and exactly segment the corneal ulcer by digital image processing and machine learning techniques, becomes an important research direction in future [1,2]. The uttermost feature of infectious keratitis is the pathogen growth in the cornea leading to focal mass cloudiness and the cornea roughness, equitably bringing out same characteristics of each pathogenic microorganism for its growth in the tissue [6]. Diagnosis of an infectious keratitis mostly depends on discriminatively find the visual features of the infectious lesion in the cornea by ophthalmologists. Clinically, ophthalmologists depend on slit lamp microscope to observe the normality or abnormality of the cornea and beyond. Besides as an observational tool, slit lamp microscope can also simultaneously be used to take a photograph and to record the existing status of the corneal manifestations for each patient visit, resulting in the growth of a well noticed dataset for an based infectious keratitis appreciation and analysis.

ISSN: 2233-7857 IJFGCN

1.1Bacterial keratitis

Bacterial:

Bacterial corneal ulcers are results from the scattering of bacteria after a violate in the corneal epithelial fence except organisms like gonococcus can penetrate an intact epithelium to cause ulcer. Factors predisposing the epithelium like corneal edema, enlarged contact lens usage, dry eyes, and trauma make it open to corneal infection. The most common microorganism is Pseudomonas Aeruginosa which utilizes glycocaluxto adhere to epithelium and then invades into the stroma through violate in epithelial. Inflammatory cells (PMNs) reach the site of corneal violate from the tears and limbal vessels which releases cytokines and interleukins resulting in progressive invasion of cornea and increase in size of the ulcer. Phagocytosis of the organism releases the free radicals and proteolytic enzymes leading to necrosis and sloughing of the epithelium, bowman's membrane and stroma. In addition, process is facilitated by proteases and exotoxin that are produced by multiplying bacteria and endotoxin that are produced by organisms after their death. The endotoxins are polysaccharides within the cell wall of gram negative bacteria and are responsible for ring infiltrates.

Symptoms:

Reduce visualizing

Tearing, Discharge, Redness are the common symptoms presented by the patients.

Pain (Disproportionate pain can be seen in Herpes and Acanthamoeba. Fungal ulcers are quieter whereas pseudomonas are fast growing)

Fig. 1 Diagnostic Approach

Fig. 2 Bacterial eye infection

ISSN: 2233-7857 IJFGCN

2. Proposed methodology

In this paper, an computerized eye aliment appreciation scheme is plan to make using various machine learning techniques..the human eye part is obtained from the facial image automatically. The first stage focusing the image.This procedure is acquired by digital camera. Initially, the original image has been loaded as an input image and then the method detects the face from the input image by our algorithm. Our method scales the facial images at 500×500 pixels. Then the method segments the various countance components. Once the eye part is segmented from the face part, we apply the eye parts of the image for learning. The phases of the proposed method are shown in Figure 3.

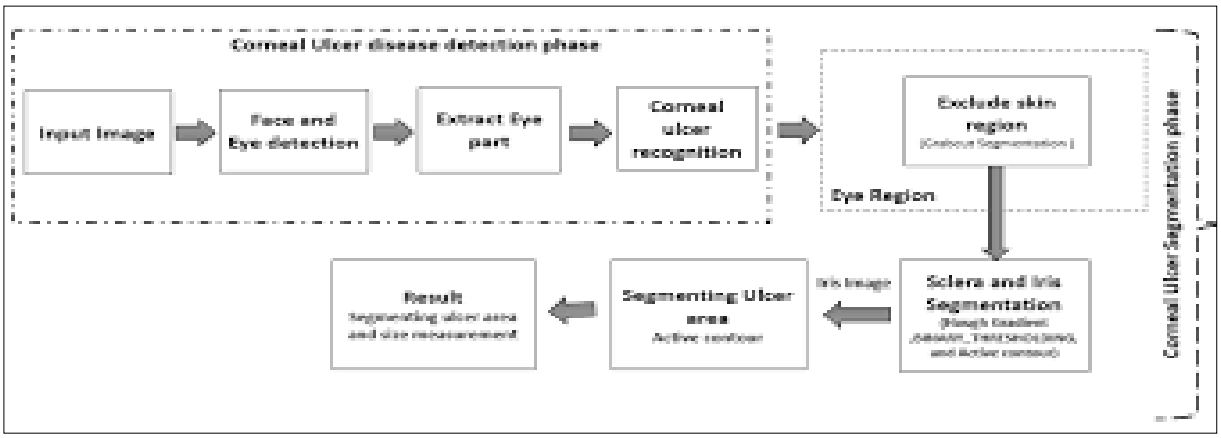

Fig. 3 Proposed Methodology

Face and Eye Detection

After face detection, eyes are the facial feature to have received the largest concentration, mostly because these play a major role in face appreciation and human-computer interaction problems. resort to highly sophisticated methods to achieve this goal [6]. A major reason behind the difficulty of detection is the high variability of these. Although most eyes may seems to be the same at first, closer analysis of a set of cropped eyes (i.e., in isolation) revels a different picture. Eyes may have very distinct shapes (mostly across ethnicity and race, but not exclusively), pupil size, and colors. Furthermore, cast shadows, glasses, and lighting have a strong influence on how eyes are seen in an image. On top of it all, eyes can be open, close or any way opened , and the iris may be pointing at any direction. For now we are interested in finding the center of the eye, regardless of the position of the iris, as well as the bounding box of the eye region . This can be considered as a first point of detection of the eye.

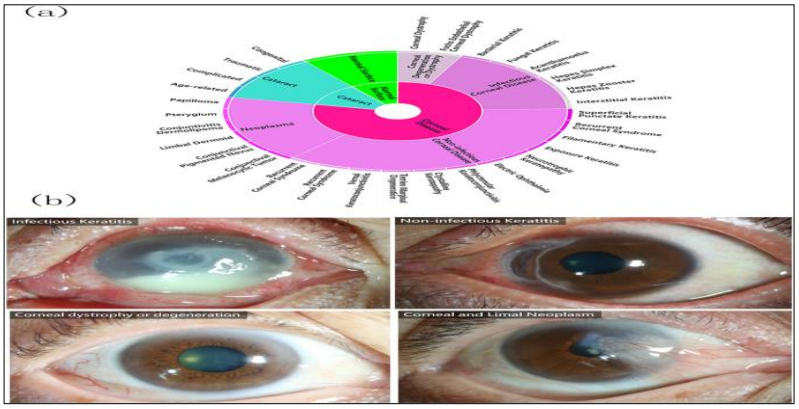

Fig. 4 First Point of Detection of The Eye

ISSN: 2233-7857 IJFGCN

2.1.1. Eye extraction

The main goal of facial feature detection is to segment the countance components, in particular for eye region extraction and segmentation. We spot and locate the position of eyes using a facial landmark detector [7].Then it converts the facial landmarks' ($x(l,i)$,$y(l,i)$)-coordinates (where l is an index of the landmark), which Specify where the 68 landmarks are. Each eye part contains six landmarks, starting at the left corner of the eyeas shown in Figure 4. For each of the eye regions, we determine the starting and ending index values to extract(x, y)-coordinates. Using these indexes we extract eye regions and scale to resolution of 70×70 pixels.

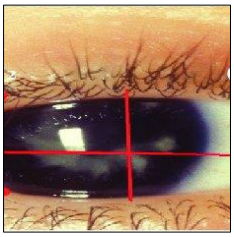

Fig. 5. Eye extraction process using facial landmarks.

2.2. Classifiers

Our Computerized eye aliment appreciation consists of several steps: facial feature extraction, ROI (region ofinterest), and feature learning. In this section, we describe our proposed machine learning methods such asdeep convolution neural network (DCNN) and support vector machine (SVM) to classify eye diseases.

2.2.1. DCNN classifier

A deep convolution neural network (DCNN) is a multilayer neural network that is performed as a deep supervised learning method [8]. The DCNN has achieved excellent effectiveness on image appreciation tasks for the last few years [9, 10, 11, 12]. It can perform both feature extraction and image classification tasks [15]. The CNN architecture has two parts: first, a many layer and a max-pool layer acting as a hierarchical feature extractor, where this feature projecting maps the input image intensitve to a feature vector, and second, a fully connected layer that performs as a classifier where the extracted features are classified. It is followed by a soft-max activation function, as they have only one output neuron for every class. Due to the DCNN'excellent effectiveness, we have proposed a method for feature extraction and disease appreciation from eye- images that uses DCNN. We have built a custom architecture for our DCNN model inspired by earlier works in [11 12] for appreciation tasks using the CNN. We mainly explore six convolution layers, six leaky ReLUs,three max-poolings, three fully combined layers, and five dropout layers. The first convolution layer receives70×70×3 (height×width×three input channels) = 14,700 input neurons associated with each pixel in the image. The values associated with each image's data matrix are normalized and fed to the hidden layer to get their classifications. The CNN-based architecture is presented in Figure 6. Table 1 shows the descriptions of the proposed CNN architecture. As shown in Figure 6,

Table 1: Descriptions of the proposed CNN architecture

Layers	Layers (type)	Feature maps and neurons	Kernel	Number of parameters
0	Input image	3@70 × 70	–	–

ISSN: 2233-7857 IJFGCN

1	Convolution	256@66 × 66	5 × 5	19456
2	LeakyReLU	LeakyReLU	–	0
3	Batch normalization	Batch normalization	–	1024
4	Convolution	256@66 × 66	5 × 5	19456
5	LeakyReLU	LeakyReLU	–	0
6	Max-pooling	256@66 × 66	2 × 2	0
7	Batch normalization	Batch normalization	–	1024
8	Dropout	0.3	–	–
9	Convolution	254@32 × 32	5 × 5	260096
10	LeakyReLU	LeakyReLU	–	0
11	Batch normalization	Batch normalization	–	512
12	Convolution	254@32 × 32	5 × 5	260096
13	LeakyReLU	LeakyReLU	–	0
14	Max-pooling	254@32 × 32	2 × 2	260096
15	Batch normalization	Batch normalization	–	512
16	Dropout	0.2	–	–
17	Convolution	127@32 × 32		130048
18	LeakyReLU	LeakyReLU	–	0
19	Batch normalization	Batch normalization	–	1024
20	Convolution	127@3 2× 32	5 × 5	130048
21	LeakyReLU	LeakyReLU	–	0
22	Max-pooling	127@32 × 32	2 × 2	0
23	Batch	Batch normalization	–	1024

ISSN: 2233-7857 IJFGCN

	normalization			
24	Dropout	0.3	–	–
25	Flatten	256	–	
26	Dense	512	Sigmoid(activation)	131584
27	Batch normalization	Batch normalization	–	2048
28	Dropout	0.5	–	–
29	Dense	256	Sigmoid(activation)	
30	Batch normalization	Batch normalization	–	1024
31	Dropout	0.5	–	–
32	Dense	8		2056
33	Softmax	8		
34	Classification output	Categorical Cross entropy	–	–

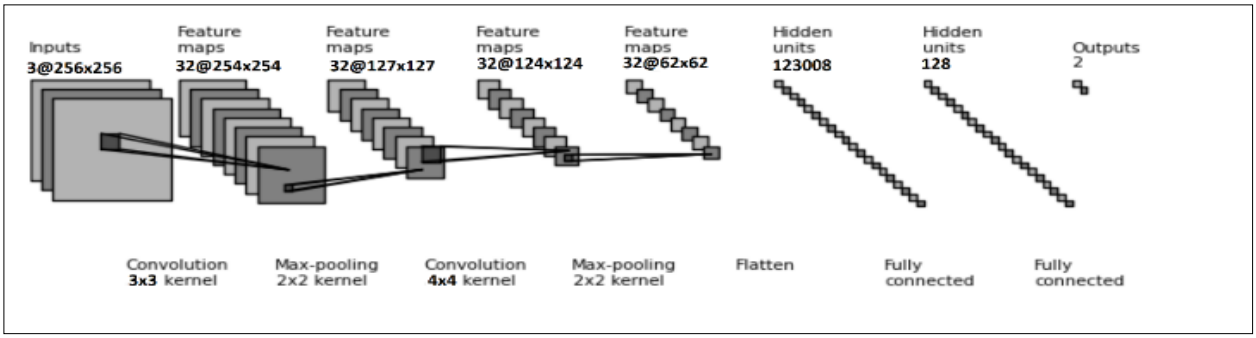

Fig.6 The architecture of the CNN.

The convolutional layer performs the mapping as follows:

$C^{s}_{(x,y)} = I_{p\times q} * W^{s}_{m.n}$ ----------*Equation 1*

Each entry of $C^{s}_{(x,y)}$ can be defined as shown in Equation 2 ^{m,n}

$$Cs(x,y)(i,j) = \sigma(\Sigma mu=i\Sigma nv=jIp\times q(u-i)(v-j) * Wsm,n(u,v) + bs):$$

ISSN: 2233-7857 IJFGCN

Here, σ is a nonlinear function. The result passes through the leaky ReLU. Although in CNN architectureReLU is the most used activation function, in our proposed architecture leaky ReLU activation is applied to solve the problem of dying neurons during back ropagation with gradient value of 0.1. The feature extractor with activation function leaky ReLU produced features vectors that consistently outperformed the feature extractors with other activation functions. We build several dropout layers to reduce model over fitting. The output of the countinuation layer is a 2D vector, which flattens into a single dimensional vector that is used as an input layer with three fully connected layers. . the fully connected layer, performs the classification followed by a softmax activation function [11]. For an input sample x, weight vector W, and K distinct linear functions, the softmax function can be defined for the *i* th class as follows:

$$P(y = i|x) = \frac{exp(x^T wi))}{\sum^{k}_{k=1exp(}xTwk)}$$

SVM classifier

The support vector machine (SVM) is a linear binary classifier proposed by Vapnik in 1995 [13]. It performs intelligent machine techniques for the purpose of condition monitoring and medical diagnosis using its duty succeed in the classification process. In this paper we focus on the SVM using radial basis function (RBF) kernels for solving nonlinear separable classification problems [14]. Given a supervised soft-margin classification problem and a training set of N data points $\{yi, xi\}mi=1$, where $xi\epsilon Rn$ is the *i* th input pattern and $yi\epsilon R$ is the*i* th output pattern, the SVM method aims at constructing a classifier that is defined as follows:

$$y(x) = sign(\Sigma m_{i=1}\alpha i\gamma i\, k(xi, x) + b) \quad \textbf{equation 4}$$

Here, αi and *b* are obtained from a quadratic optimization problem. The quadratic optimization problem hasa trade-off parameter C, which is defined by the experiment or user. In this paper we applied a Gaussian radial basis function (RBF) kernel that is defined as follows:

$K(xi, x) = e\gamma||xi-x||2$ equation 5

,

3 Experimental results

In this section, we describe the dataset used for eye aliment experimentation, present the experimental setup and results, analyze different machine learning algorithm settings, and then compare our method to other eye aliment appreciation techniques.

Datasets

First we develop a dataset for seven eye diseases. Images are does not depend on collected from International Centre for Eye Health,[2] clinical images for symptoms on faces from the University of Rochester [9], UCSD School of Medicine and VA Medical Center [9], the Primary Care Dermatology Society [9], and other different resources [22, 23]. Some sources contain full face

ISSN: 2233-7857 IJFGCN

images with diseases. We crop the eye parts and resize the images. Allimages are resized to 256 × 256. The dataset contains 1753 images. Table 2 shows the statistics of the image dataset. Figure 6 shows some image samples from our dataset. The symptoms of selected eye aliment include several visual abnormal in the eye region, particularly not clear or clouded or yellowing lens, gray or white spots on the cornea, red or bloodshot eyes, yellow or greenish-yellow coatings on eyes, white spots in sclera, swollen eyes, eyelid deformity such as the length of the lower eyelid being turned out from the eye, or reddish bumps on the edge of an inner eyelid depending on specific aliment and symptoms are different foreach aliment.

Experimental setup and results

The entire experiment was conducted on a system with an Intel Core i7-7700HQ, an additional GPU (NVIDIA GeForce GTX 1060, 6 GB GDDR5), 512 GB SSD memory, and Keras with Tensorflow on the back end. All the model's results were implemented using OpenCV and Python. The facial landmark detector with pretrained models are used to evaluate the 68 landmarks of facial structures on the face image [16].The facial landmark extraction method uses the iBUG 300-W dataset for training [16]. This dataset comprises 135 images with 68 landmarks including different poses, lighting conditions, subjects, etc.

We conduct comparativetesting for eye aliment with DCNN and SVM method on our dataset.

Table 2. Statistics of image dataset.

Images	Number of images
Corneal ulcer	360
Ectropion	211
Cataracts	186
Conjunctivitis	250
Trachoma	122
Periorbital cellulitis	167
Bitot's spot of vitamin A deficiency	189
Healthy	269
Total images	1753

too large for preprocessing efficiently. We have resized all the eye aliment images to 70 × 70 pixels to reduce the time of training that was evaluated by script in Python, using Keras and the OpenCV framework. To reduce biases in the feature selection of the validation set, we perform a 10-fold cross-validation technique on the dataset. In 10-fold cross-validation, the original dataset is randomly divided into ten equallysized subsets. Then, each time, a single subset is used as the validation set and nine other subsets are used fortraining with 40 epochs each. Here, 20% of the original images

ISSN: 2233-7857 IJFGCN

are reserved as a test set, and 1402 images are randomly selected from the remaining dataset for training our models at the starting point. The DCNN model identifies 334 images out of 360 eye images correctly. From the experimental results of the DCNN model we see that the average accuracy rate is 98.79% with specificity of 97% and sensitivity of 99%. To evaluate the CNN model's performance, several performance metrics are used such as accuracy, precision, recall, and F-score as shown in Table 3. Figure 7 depicts the CNN model's accuracy and loss with the number of epochs, resulting in

a mean error rate of the proposed system of 3%.

Table 3. Statistical results of CNN model.

Model		Precision	Recall	F-score	Accuracy % (cross-validation [k=10])	Average model accuracy % (cross-validation [k=10])
CNN model	Bitot's spot of vitamin A deficiency	1.00	0.95	0.97	99.43	98.79
	Cataracts	1.00	0.95	0.97	99.43	
	Conjunctivitis	1.00	0.94	0.96	98.86	
	Corneal ulcer	0.94	1.00	0.95	98.27	
	Ectropion	0.97	0.98	0.94	98.58	
	Periorbital cellulitis	1.00	0.82	0.90	98.29	
	Trachoma	1.00	0.88	0.93	99.15	
	Healthy eye	0.90	1.00	0.95	98.29	

In order to get the other three solution, the proposed system uses hybrid features of SVM for recognition of seven eye aliment. We propose the RBF kernel-based support vector machine [13] with three different models such as the SVM model, PCA-SVM model, and t-SNE–SVM model. We test our dataset with

ISSN: 2233-7857 IJFGCN

Figure 6. Sample images of eye diseases and healthy eyes.

SVM, PCA-SVM, and t-SNE–SVM models. The PCA and t-SNE are used for feature selection of segmented eyes from images and decreasing the feature matrix size by selecting the most required features. We compare among these models with performance metrics such as accuracy, precision, recall, and F-score as shown in Table.We select the range of parameter C and the value of γ and apply a 10-fold cross-validation technique on our dataset using the SVM with RBF kernel.

The grid searching range of the SVM in each parameter is C = $[2^{-2} \ldots\ldots 2^{7}]$ and γ = $[2^{-7} \ldots\ldots 2^{2}]$. Inall combinations of SVM models tried we have 10 * 10=100 different combinations. We have achieved the best accuracy rate for C = 14.444 and γ = 0.008 in the SVM, PCA-SVM, and t-SNE–SVM models. These parameters are then used to train and test these three models. The SVM model without PCA is able to attempt an average accuracy rate of 91.70% with sensitivity of 91% and specificity of 94%. The PCA-SVM model

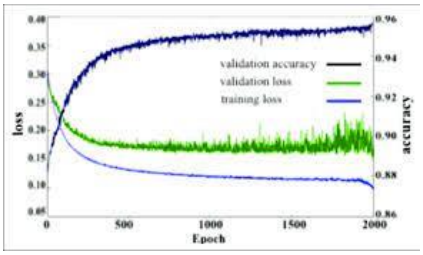

Fig. 7 SVM with RBF kernel

We also compute specificity and sensitivity, defined as follows:

True positives (TP), true negatives (TN), false positives (FP), and false negatives (FN) are vital to understanding the evaluation of disease diagnosis. A true positive (TP) is defined as the patient having an eye disease that was successfully detected as the selected eye disease image. A false positive (FP) is defined as a patient not having the eye disease but being detected as having the eye disease symptoms, true negative (TN) is defined as the patient not having the eye disease and being

ISSN: 2233-7857 IJFGCN

detected as a healthy eye image, and a false negative (FN) is defined as the patient having the eye disease but the eye disease not be recognized. Table 5 shows the specificity and sensitivity of the proposed model. The proposed CNN model obtained the highest sensitivity rate of 97% and specificity of 99%. The t-SNE-SVM-based model shows the lowest sensitivity rate of 13% and specificity of 88%. From the results, sensitivity and specificity are improved by the proposed system. Moreover, we see that the results of our methods are better than those of other eye disease finiding systems.

Table 5. Comparison of statistical results of proposed machine learning techniques.

	CNN				SVM				PCA-SVM				T-SNE-SVM			
	TP	FP	Sensitivity	Specificity	TP	FP	Sensitivity	Specificity	TP	FP	Sensitivity	Specificity	TP	FP	Sensitivity	Specificity
Bitot's spot of vitamin A deficiency	35	0	0.95	1.00	35	0	0.95	1.00	35	0	0.95	1.00	0	0	0	1.00
Cataracts	35	0	0.99	1.00	37	19	1.00	0.94	37	14	1.00	0.96	0	0	0	1.00
Conjunctivitis	47	1	1.00	0.99	50	0	0.98	1.00	50	0	1.00	0.98	0	0	0	1.00
Corneal ulcer	74	6	1.00	0.98	74	0	1.00	1.00	74	0	1.00	0.97	74	274	1.00	0.01
Ectropion	41	4	0.98	0.99	42	0	0.88	0.91	42	0	1.00	1.00	0	0	0	1.00
Periorbital cellulitis	27	0	0.94	1.00	25	0	0.96	0.86	27	0	0.96	1.00	0	1	0	0.99
Trachoma	21	0	0.89	1.00	17	0	0.76	0.82	18	0	0.82	1.00	0	0	0	0.99
Healthy eye	54	6	1.00	0.98	52	0	0.71	1.00	52	0	0.75	1.00	0	2	0	1.00

Figure 8 shows the ROC curve calculated with the true positive and false positive statistical features from Table 5. The fitted ROC areas for the proposed systems are 0.99, 0.99, and 0.50 for the SVM, PCA-SVM, and t-SNE-SVM models, respectively. Here class 0, class 1, class 2, class 3, class 4, class 5, class 6, and class 7 are Bitot's spot of vitamin A deficiency, cataracts, conjunctivitis, corneal ulcer, ectropion, healthy, periorbital cellulitis, and trachoma, respectively. The ROC area shows the overall performance of the algorithm. Results show that the image of an

ISSN: 2233-7857 IJFGCN

eye is classified as aliment or healthy.In Table 6,

.

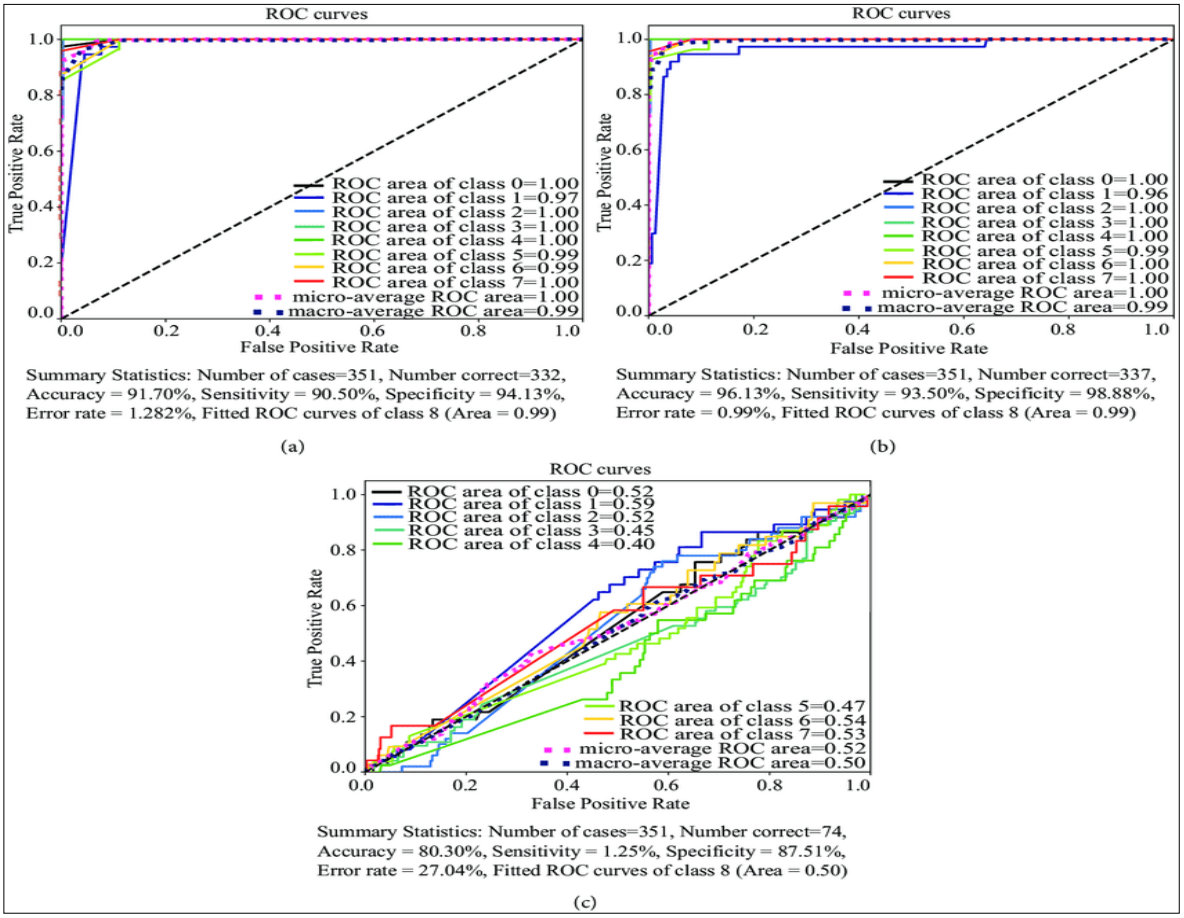

Fig. 8 ROC curve

Conclusion

In this paper, we propose a visual content-based eye aliment appreciation scheme from facial images using image processing and machine learning techniques. In this paper we have developed visual content- based image dataset for seven eye diseases containing data of 1753 images. Our proposed system is based on an algorithm that automatically crops the eye part from a frontal facial image. These eye parts are used for learning. We apply two learning methods for classification: DCNN and SVM. We also apply PCA and t-SNE for feature selection and then classify by SVM. We test our system with seven eye aliment that are seen . From the experimental setups we see that DCNN outperforms SVM models. Of the SVM models, the PCA-SVM model shows good results than the other two SVM models. We also compare to test the appreciation accuracy of DCNN methods. It is observed that our method achieves better accuracy than others. We get a recognition rate of our method of 98.79% with sensitivity of 97% and specificity of 99%.

REFERENCES

[1] B.T. Lopes, A. Eliasy, and R. Ambrosio, “Artificial Intelligence in Corneal Diagnosis: Where Are we?,” *Current OphthalmologyReports*, Vol. 7 Issue 3, pp. 204–211, July 2019. .

ISSN: 2233-7857 IJFGCN

[2] P. Manikandan, A. Abdel-hadi, Y. Randhir Babu Singh, R. Revathi, R Anita et al. "Fungal Keratitis: Epidemiology, Rapid Detection, andAntifungal Susceptibilities of Fusarium and Aspergillus Isolates fromCorneal Scrapings," BioMed research international, 2019.

[3]U. Gopinathan, P. Garg, M. Fernandes, S. Sharma, S. Athmanathan, and G. N. Rao, "The epidemiological features and laboratory results of fungal keratitis: a 10-year review at a referral eye care center in south india," *Cornea*, vol. 21, no. 6, pp. 555–559, 2002.

[4]Sharma S, Garg P, Rao GN. Patient characteristics, diagnosis, and treatment of non-contact lens related Acanthamoeba keratitis. Br J Ophthalmol. 2000;84(10): 1103-1108.

[5]. Khor WB, Prajna VN, Garg P, et al. The Asia Cornea Society Infectious Keratitis Study: A Prospective Multicenter Study of Infectious Keratitis in Asia. Am J Ophthalmol. 2018;195:161-170.

[6] T. Moriyama, T. Kanade, J. Xiao and J.F. Cohn, "Meticulously Detailed Eye Region Model and Its Application to Analysis of Facial Images," PAMI 28:738-752, 2006. 1, 2, 3 [11] M.

[7]Pantic and L.J.M. Rothkrantz, "Automatic analysis ofKazemi V, Sullivan J. One millisecond face alignment with an ensemble of regression trees. In: 2014 IEEEConference on Computer Vision and Pattern Recognition; Columbus, OH, USA; 2014. pp. 1867-1874. doi:10.1109/CVPR.2014.241

[8] Hinton GE, Salakhutdinov RR. Reducing the dimensionality of data with neural networks. Science 2006; 313 (5786):504-7. doi: 10.1126/science.1127647

[9] Esteva A, Kuprel B, Novoa RA, Ko J, Swetter SM et al. Dermatologist-level classification of skin cancer with deepneural networks. Nature 2017; 542 (7639): 115–118. doi: 10.1038/nature21056

[10] Gargeya R, Leng T. Automated identification of diabetic retinopathy using deep learning. Ophthalmology 2017;124 (7): 962-969. doi: 10.1016/j.ophtha.2017.02.008

[11] Esteva A, Kuprel B, Novoa RA, Ko J, Swetter SM et al. Dermatologist-level classification of skin cancer with deep neural networks. Nature 2017; 542 (7639): 115–118. doi: 10.1038/nature21056

[12] Gargeya R, Leng T. Automated identification of diabetic retinopathy using deep learning. Ophthalmology 2017;124 (7): 962-969. doi: 10.1016/j.ophtha.2017.02.008

[13] Cortes C, Vapnik V. Support-vector networks. Machine Learning 1995; 20 (3): 273–297. doi:10.1023/A:1022627411411

[14] Rajkumar N, Jaganathan P. A new RBF kernel based learning method applied to multiclass dermatology diseasesclassification. In: 2013 IEEE Conference on Information & Communication Technologies; Thuckalay, India; 2013.pp. 551-556. doi: 10.1109/CICT.2013.6558156

[15] Sagonas C, Tzimiropoulos G, Zafeiriou S, Pantic M. A semi-automatic methodology for facial landmark annotation.In: CVPRW '13 Proceedings of the 2013 IEEE Conference on Computer Vision and Pattern Recognition Workshops;Washington, DC, USA; 2013. pp. 896-903. doi: 10.1109/CVPRW.2013.132

[16] Sagonasa C, Antonakosa E, Tzimiropoulosb G, Zafeiriou S, Pantic M. 300 faces in-the-wild challenge: database andresults. Image and Vision Computing 2016; 47: 3-18. doi: 10.1016/j.imavis.2016.01.002932

ISSN: 2233-7857 IJFGCN